TITLE: Selection of healing agents for a vascular self-healing application.

AUTHORS: A. Cuvellier[a], A. Torre-Muruzabal[a], G. Van Assche[a], K. De Clerck[b] and H. Rahier[a].

AFFILIATIONS:

a: Physical Chemistry and Polymer Science (FYSC), Department of Materials and Chemistry, Faculty of Engineering, Vrije Universiteit Brussel (VUB), Pleinlaan 2, B-1050 Brussels, Belgium

b: Fiber and Colouration Technology Research Group, Department of Textiles, Faculty of Engineering and Architecture, Ghent University, Technologiepark 907, 9052 Ghent, Belgium

ABSTRACT:

To increase the durability and reliability of thermosets, self-healing via a vascular network, is developed. A judicious choice of healing agents proves to be necessary to achieve the best recovery of properties. Four low viscosity two-component epoxy-amine healing systems were compared, to check which glass transition temperature range would be best to recover mechanical properties (T_g ranging from -8 to 68 °C). Interdiffusion experiments show that all systems react sufficiently slowly at room temperature to allow interdiffusion of epoxy and amine over more than 1 mm before the diffusion is stopped by vitrification. Swelling tests revealed that most of the selected healing agents diffuse into the surrounding matrix and swell it. This might be beneficial for crack closure and improved adhesion between healing system and matrix. Flexural tests demonstrated that, the higher the glass transition temperature of the fully cured healing system, the higher the healing capability.

KEYWORDS: self-healing polymer; vascular network; autonomous; epoxy-amine; glass transition temperature

1. INTRODUCTION

Thermosetting polymers and polymer composites have seen a significant increase in use over recent decades, due to main advantages such as light weight, good processability and chemical stability under atmospheric conditions. Despite their success, reliability and durability are still problematic for structural applications, due to the creation of microcracks as a consequence of mechanical stress and cyclic thermal fatigue in these brittle polymers. This emphasizes the need for self-healing polymers, that are able to repair themselves in an autonomous way and recover their initial functionality when the healing mechanism is triggered by a crack formed in the matrix [1–3].

The self-healing mechanism can be extrinsic or intrinsic. When extrinsic, the healing mechanism is based on healing agents, pre-embedded in capsules [3–8], hollow fibres [9–11] or vascular networks [12–15], that can be carried rapidly to the damaged site. When a crack forms it triggers the delivery of the healing agents and allows autonomic healing without manual intervention [1,16]. When intrinsic, the self-healing mechanism is inherent to the chemical nature of the polymer and doesn’t require major external input such as vascules, but

generally an external stimulus (heat [17,18], light [19,20], ...) is required, often making the system non-autonomic.

Capsule-based self-healing systems are by far the most studied, but have a few important drawbacks, such as the inability of repeated healing at a given location [21,22], the large size of the capsules (10-1000µm) [23] and the large volume fraction of microcapsules needed to heal cracks at an early stage. Moreover, achieving the required dispersion of the microcapsules and/or the catalyst to cover the whole substrate can be problematic [24]. In contrast, vascular networks permit repeated healing in the same location, and allow the healing agents to reach more distant points of the substrate, thus increasing the available volume of healing agent to repair a crack, and could in principle replenish the system. Some vascular systems with channel diameters between 200 µm to 2.5 mm have been discussed in literature [12,25,26]. The large channels, however, reduced the mechanical properties of the material.

The overall objective is the development of an autonomous self-healing polymer that uses a vascular network of submicron (830 ± 130 nm) channels. In this paper, the focus will be on the selection of a two-component epoxy-amine healing chemistry to autonomously self-heal an epoxy thermoset. Although epoxy-amine systems for self-healing [7,27,28] have been extensively studied, only few studies compared several epoxy-amine pairs [29] and to our knowledge none studied the influence of Tg of the healing system on the healing capability, when autonomic healing at ambient temperature. The healing agents are combined in healing systems for which the glass transition temperatures at full cure ($T_{g\ x=1}$) are below, around and above room temperature, to study the influence of the $T_{g\ x=1}$ of the healing system on the healing capability. x=1 indicates that full conversion is reached, and thus that at least one of the reagents is depleted.

2. MATERIALS

Triethylenetetramine (TETA), poly(propylene glycol) diglycidyl ether (PPGDE) and trimethylolpropane triglycidyl ether (TMPTE) were purchased from Sigma Aldrich, Jeffamine D 230 polyetheramine (JEFF D230) and Jeffamine D 400 polyetheramine (JEFF D400) were from Huntsman. These epoxy resins and amines were used in different combinations for the healing systems. The chemical structure, purity, viscosity and molar mass of the healing agents are given in Table 1. The original epoxy thermoset matrix was prepared using RIMR 135 Epikote resin (mainly contains diglycidyl ether of bisphenol A) and RIMH 137 Epikure curing agent (mainly contains alkyletheramines and isophorone diamine) in a 100:30 weight ratio, both purchased from Hexion. Food-grade pullulan with a molar mass of 200 kDa and a density of 1.85 g.cm^{-3}, kindly provided by Hayashibara Biochemical Laboratories Inc., was used to prepare electrospun submicron polysaccharide fibres.

Abbreviation	Structure	Molar mass (g.mol^{-1})	Viscosity (mPa.s)	Purity (%)

TETA	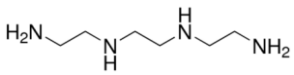	146	20	70
JEFF D230	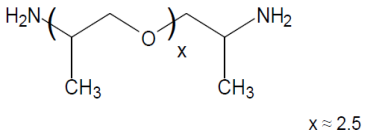 x ≈ 2.5	230	9	Min 97%
JEFF D400	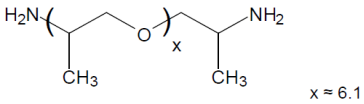 x ≈ 6.1	430	22	Min 97%
PPGDE	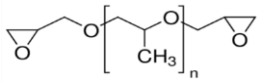	380	30-60	n.a.
TMPTE	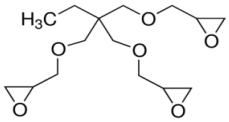	302	120-180	n.a.

Table 1:Structure, molar mass (g.mol-1), viscosity (mPa.s) and purity of the different healing agents.

3. EXPERIMENTAL

3.1 Preparation of the vascularised thermosets

The vascular network was prepared by embedding electrospun sacrificial polysaccharide (pullulan) fibres into the thermoset epoxy matrix. To electrospin the fibres, the polymer solution (25 wt% of pullulan) was pumped with a flow rate of 1 $mL.h^{-1}$ through a nozzle with an inner diameter of 1.024 mm. The tip to collector distance was 20 cm and the voltage was varied between 15 and 30 kV. The setup is composed of a voltage source (Glassman High Voltage Series EH30P3), an infusion pump (KD Scientific Syringe Pump Series 100), and a grounded collector plate, and is operated in a climate chamber (Weiss WK 340/40). The solution was electrospun at 23 ± 1.5 °C and 50 ± 3% relative humidity. For the thermoset epoxy matrix, RIMR135 and RIMH137 were mixed for about 10-15 minutes and degassed under vacuum. Mats of electrospun polysaccharide fibres were placed in the mould in between peel plies and glass fibre meshes. Next, the fibre mats were impregnated with resin by vacuum-assisted resin transfer. The composites were cured for 24 h at ambient temperature and subsequently post-cured for 15 h at 80 °C to obtain an epoxy with a glass transition temperature of 87°C. After curing, samples of the required dimensions were cut from the cured composite plate (300 mm x 300 mm x 3 mm). The polysaccharide fibres were dissolved by immersing the composite pieces in water under stirring, leaving a network of interconnected submicron channels behind (Figure 1). More details can be found in [30].The samples discussed in this paper contained 9 vol% of channels that were 830 ± 130 nm wide. Samples of virgin (non-vascularized) epoxy thermoset were prepared using the same curing conditions and cut to the required size.

FIGURE 1(double column)

3.2 Methods

DSC experiments were performed on a DSC Q2000 from TA instruments. Nitrogen was used as a purge gas, with a flow rate of 50 $ml.min^{-1}$. A T4P calibration was performed using sapphire, and temperature and enthalpy were calibrated using indium.

To measure the glass transitions at full cure ($T_{g\ x=1}$) of the healing systems, samples were cured 4 days at room temperature and 15 hours at 50°C. For the TETA/TMPTE system, an additional post cure of 5 hours was done at 80°C to reach full cure. Determination of $T_{g\ x=1}$ was done using a modulated temperature experiment with a modulation amplitude of 0.25 K and period of 30 s, at a heating rate of 2.5 $K.min^{-1}$ from -70°C to 100°C.

Microcalorimetry experiments were performed under isothermal conditions at 25 °C using a TA Instruments TAM III. To study the reaction kinetics, samples of mixed healing agents (mass between 1-1.15 g) were introduced into 4 mL glass ampoules. When performing microcalorimetry, the sample was first introduced in an equilibration position for 15 minutes, and then moved into the measuring position inside one of the microcalorimeter channels. The data points recorded over the first 45 minutes are considered unreliable due to the slow response of the device. For fast reactions, this implies a non-negligible amount of heat flow is not correctly measured, which is why the estimated initial heat flow value is obtained by extrapolation for the first hour of reaction. This heat is then added to the measured heat, determined by integration. From this value (in $J.g^{-1}$), the heat of reaction ($kJ.mol^{-1}$), is calculated by dividing by the concentration of reactive functional groups (epoxy or N-H) in $mol.g^{-1}$ of the healing agent that will be depleted first.

To study interdiffusion, samples with healing agents (total mass of 4 g) gently deposited one on top of the other (Figure 2), in 20 mL glass ampoules, were prepared by adding the second component along the wall of the ampoule to avoid mixing. Samples with amine on top and epoxy on top were prepared. The heat release resulting from interdiffusion and reaction was followed at 25 °C over the course of several days using a TAM Air. The larger glass ampoules used in this system permit a larger contact area between the two reagent phases than when using 4 mL ampoules and the TAM III.

FIGURE 2 (single column)

The infusion of the healing agents into the vascular network by capillary forces was followed by monitoring the weight of the sample using a TA Instruments TGA 2950. The sample was hung from the hangdown wire with the bottom in contact with the liquid in a wide beaker to ensure a negligible decrease in liquid level. The uptake of amine and epoxy was done on separate samples.

Fourier transform infrared spectroscopy (FTIR) analysis was done using a FTIR Nicolet 6700 with Smart iTR Attenuated Total Reflectance (ATR) sampling accessory with a diamond-coated ZnSe crystal. FTIR was used to determine whether the wicking of the samples only occurs at the inside or also at the outside of the sample. This was done by positioning an infused sample on the ATR crystal at a location that was not immersed in the healing agent.

Dynamic mechanical analysis (DMA) measurements were performed using a DMA Q800 from TA instruments. Due to the rubbery character of some of the samples, a dual cantilever set-up was chosen (span 35 mm). Samples of 50 mm long, 5 mm wide and thickness between 3.0 and 3.5 mm were measured in multi-frequency-strain mode, using a frequency of 1 Hz, with a strain between 0.1% and 0.3% for samples in rubbery state and between 0.03% and 0.08% for the samples in glassy state. The samples were heated at a rate of 2.5 $K.min^{-1}$ over a temperature range of at least 150°C. The samples were cured in the same way as mentioned above for the $T_{g\ x=1}$ determination.

To evaluate the healing capacity of the different healing systems, virgin thermoset samples were broken and glued back together by putting a drop of mixed healing agents onto the fracture surfaces, and bringing the pieces back together, applying slight pressure, using a set-up specially designed for this purpose, for 7 days at ambient temperature. Flexural tests were performed using a three-point-bending setup on an Instron 5885H, following ISO 178:2010 [31]. The specimens were 60.8 mm long, 12.7 mm wide and 3 mm thick. The span length was 47.4 mm, and the strain rate 0.01 $mm.mm^{-1}.min^{-1}$. The healing capability is calculated by taking the ratio of the peak load for the samples healed with the amine/epoxy healing system over the peak load of samples healed with the original thermoset matrix mixture and fully cured. The values mentioned are the average of at least 3 measurements.

4. RESULTS AND DISCUSSION

4.1 Glass transitions

In vascular self-healing approaches based on two component healing systems, both components leak into the crack plane or damage site, where they will mix, react and restore the material properties. To determine the influence of $T_{g\ x=1}$ of the healing system on the healing capability, low viscosity amines and epoxies were combined into healing systems with $T_{g\ x=1}$ for stoichiometric ratios below, around and above 25 °C. As the mixing of the reagents in the crack plane is not controlled and the ratios of amine and epoxy might be off-stoichiometric, $T_{g\ x=1}$ measurements were performed for stoichiometric and off-stoichiometric amine/epoxy ratios using DMA and DSC. The measurements were performed for amine/epoxy ratios ranging from 0.7-1 to 1.3-1. From the DMA results (Figure 3), it can be seen that JEFF D230/PPGDE and JEFF D400/TMPTE systems have a $T_{g\ x=1}$ below 25 °C, JEFF D230/TMPTE around 25 °C, and TETA/TMPTE above 25 °C. The results show that, for all systems except the TETA/TMPTE, the maximum in $T_{g\ x=1}$ is at the stoichiometric amine/epoxy ratio (r = 1-1). However, for TETA/TMPTE this is at a r = 1.1-1 ratio. In general, the more off-stoichiometric the system is, the lower the values for $T_{g\ x=1}$ will be. These results are in agreement with the DSC data (Table 2). This implies that a system with $T_{g\ x=1}$ above 25 °C for a stoichiometric ratio, will have a $T_{g\ x=1}$ below 25 °C if the ratio is sufficiently off-stoichiometric. This is important with respect to the occurrence of vitrification and diffusion-controlled cure [32].

FIGURE 3 (double column)

The decrease in $T_{g\ x=1}$ for off-stoichiometric ratios can be explained by the decrease in crosslink density, or the increase in the molar mass of the segments between the crosslinks, which leads to an increase in free volume, and thus segmental mobility will be gained at lower temperatures [33]. The molar mass of the segments between crosslinks (M_c in g.mol^{-1}) of the fully cured healing systems was estimated from the storage modulus at $T = T_g + 30$ K in the rubbery plateau, with T_g the temperature at the maximum of the loss modulus, according to [34]

$$M_c = \frac{\rho RT}{G'} \quad (1)$$

with ρ (=1.12 g.cm^{-3}) the density of the polymer, R the universal gas constant, T (K) the temperature at $T = T_g + 30$ K, and with G' (in MPa), the real component of the shear modulus, given by [35]:

$$G' = \frac{E'}{2(1-\nu)} \quad (2)$$

with E' (in MPa) the storage modulus measured in the rubber plateau at $T = T_g + 30$ K and ν the Poisson coefficient (0.44 [36,37]).Table 2 indeed indicates a lower value of M_c for systems with higher T_g. The TETA/TMPTE system that showed its highest $T_{g\ x=1}$ at r = 1.1-1, shows its lowest M_c (and highest E' at T_g + 30 K) at the same ratio.

Finally, T_g decreases more when there is an excess of epoxy than when there is an excess of amine. A similar trend can be seen for E' at 25°C and at T_g + 30 K. This can be explained based on the functionality of the amines and epoxies. The studied epoxies are bifunctional and trifunctional, whereas the studied amines are tetrafunctional and hexafunctional. When a bifunctional epoxy is considered then each unreacted epoxy group due to a shortage of amine N-H groups will lead to a dangling chain end, lowering T_g. A similar shortage of epoxy groups will lead to fewer dangling chain ends, since amines connected in only two of their four or six functionalities will still be part of the network.

r (-)	$T_{g\ DSC}$ (°C)	$T_{g\ DMA}$ (°C)	$E'_{25°C}$ (MPa)	$E'_{Tg + 30\ K}$ (MPa)	$G'_{Tg + 30\ K}$ (MPa)	M_c (g.mol^{-1})
JEFF D230/PPGDE						
0.7-1	-26	-27	0.7	1.1	0.4	6700
0.8-1	-23	-20	1.7	1.6	0.6	4700
0.9-1	-13	-13	2.3	2.4	0.8	3300
1-1	-8	-8	3.7	3.7	1.3	2100
1.1-1	-9	-10	3.2	3.4	1.2	2300
1.2-1	-11	-10	2.4	2.7	0.9	2900
1.3-1	-13	-16	1.6	2.2	0.8	3500

JEFF D400/TMPTE						
0.7-1	-6	-9	3.1	3.3	1.1	2400
0.8-1	-4	-4	4.2	4.1	1.4	2000
0.9-1	0	1	6.8	5.9	2.0	1400
1-1	3	5	12	9.5	3.3	870
1.1-1	1	2	7.6	6.9	2.4	1200
1.2-1	-1	-1	6.5	5.9	2.0	1400
1.3-1	-3	-5	5.0	5.0	1.7	1600
JEFF D230/TMPTE						
0.7-1	11	4	9	6.6	2.3	1200
0.8-1	13	15	37	7.5	2.6	1100
0.9-1	23	21	270	9.9	3.4	880
1-1	28	28	930	16	5.6	550
1.1-1	25	24	420	11	3.8	800
1.2-1	21	21	88	6.8	3.8	800
1.3-1	15	15	31	8.1	2.6	1100
TETA/TMPTE						
0.7-1	57	/	1900	39	13	/
0.8-1	59	48	2200	40	14	240
0.9-1	66	51	2400	43	15	220
1-1	68	57	2500	47	16	210
1.1-1	66	63	2400	52	18	190
1.2-1	63	62	2400	52	18	190
1.3-1	62	61	2300	50	17	200

Table 2: DMA results for the different healing systems: r the amine/epoxy ratio, Tg DSC the glass transition temperature at full cure determined by DSC, Tg DMA the glass transition temperature determined from the maximum in the loss modulus, E' the storage modulus at 25 °C and at T=Tg + 30 K, G' the real component of the shear modulus at Tg + 30 K, and Mc the estimated molar mass of the segments between the crosslinks.

4.2 Isothermal cure kinetics

To study the cure kinetics of the different healing systems, isothermal microcalorimetry measurements were performed at 25°C on the mixed healing agents. The heat flow released by the samples, which is proportional to the reaction rate or the consumption rate of epoxy groups, is given as a function of time in Figure 4. TETA/TMPTE reacts the fastest, with a maximum heat flow that is 5 times larger than for JEFF D230/TMPTE and JEFF D230/PPGDE, and about 10 times larger than for JEFF D400/TMPTE. After 2, 4, 7 and 9 days, 95% of the heat of reaction has been released for TETA/TMPTE, JEFF D230/TMPTE, JEFF D230/PPGDE and JEFF D400/TMPTE, respectively.

FIGURE 4 (single column)

The measured reaction enthalpy, given per mol of minority component in Table 3, is similar for JEFF D230/PPGDE, JEFF D230/TMPTE, and JEFF D400/TMPTE and is about -109 kJ.mol^{-1} for the off-stoichiometric ratios and -101 kJ.mol^{-1} for the stoichiometric ratios. This is in agreement with the values found in literature, which are between -122 to -98 kJ.mol^{-1} of reacted epoxy functionality [38–40]. For these systems, the lower reaction enthalpies for the stoichiometric ratios are probably due to steric hindrance at the highest conversions,since topological restrictions may prevent residual unreacted groups to meet and react.

Amine/epoxy ratio	$-\Delta_r H$ (kJ.mol^{-1})
JEFF D230/PPGDE	
0.8-1	109
1-1	102
1.2-1	108
JEFF D400/TMPTE	
0.8-1	108
1-1	101
1.2-1	109
JEFF D230/TMPTE	
0.8-1	110
1-1	99
1.2-1	110
TETA/TMPTE	
0.8-1	98
1-1	91
1.2-1	99

Table 3: Reaction enthalpy for the different healing systems for stoichiometric and off-stoichiometric amine/epoxy ratios as measured by microcalorimetry. The error on these values is about 5%.

The TETA/TMPTE shows lower values for the reaction enthalpy for all ratios: about -98 kJ.mol^{-1} for the 0.8-1 and 1.2-1 ratios, and even only -91 kJ.mol^{-1} when stoichiometric. This is related to the full cure T_g, which is below or around 25 °C for the first three systems, and well above 25 °C for TETA/TMPTE (Figure 3d). Consequently, when cured at 25°C, the TETA/TMPTE system will vitrify gradually as T_g approaches and crosses the cure temperature. Upon vitrification, the segmental mobility slows down markedly, the polymerization reaction becomes diffusion-controlled. As a result, the final conversion will not reach 100% at 25 °C.

4.3 Interdiffusion and reaction experiments

Microcalorimetry was also used to study the interdiffusion and concurrent reaction between the healing agents. When channels of both healing agents are damaged by the progress of a crack, healing agents will leach out, diffuse into each other and start polymerizing. The increasing polymerization and cross-linking will slow down the diffusion of unreacted healing agents. Isothermal experiments were performed at 25 °C on layered samples, which were prepared by putting the healing agents gently on top of one another, by adding the second component along the ampoule wall, such that they did not mix. This was done both for the amine on top of the epoxy and the epoxy on top of the amine. Due to the difference in density,

the epoxy formed the bottom layer regardless of the order in which they were added. By adding the epoxy along the wall, when it is added as the second component, the additional interaction between the epoxy and amine was minimized, and thus this did not significantly influence the thickness of the formed layer and the ratio of heat of reactions. In Table 4, the average values of both configurations were taken. JEFF D230/PPGDE and TETA/TMPTE have a similar heat of reaction ratio of about 40%, whereas this is less than 30% for JEFF D230/TMPTE and JEFF D400/TMPTE. This means that, for JEFF D230/PPGDE and TETA/TMPTE, diffusion takes place over a larger distance, allowing more reaction than for JEFF D230/TMPTE and JEFF D400/TMPTE. This can be explained by the fact that TETA is the amine with the lowest molar mass (146 $g.mol^{-1}$, compared to 230 $g.mol^{-1}$ and 430 $g.mol^{-1}$ for JEFF D230 and JEFF D400, respectively) and that it has no side groups, while PPGDE is larger than TETA but more linear than TMPTE, which has more a bulky (3D) structure.

After reaction, the thickness of the solid layers formed within the bottles was measured (Table 4) after being removed from the bottles and cleaned. The measured thicknesses give an underestimation of how far the diffusion-reaction process progressed, as only the distance over which gelation has occurred is measured. Diffusion did occur over larger distances; however, in locations where gelation has not been reached, the resin is still liquid and will be wiped away. The thickness of the solid layers was very similar for JEFF D230/PPGDE, JEFF D230/TMPTE and JEFF D400/TMPTE, and varied between 1.2 mm and 1.3 mm, whereas the thickness for TETA/TMPTE was about 3.1 mm.

	$\Delta H_{layers}/\Delta H_{mixed}$ (%)	Thickness (mm)
JEFF D230/PPGDE	39	1.3
JEFF D400/TMPTE	24	1.2
JEFF D230/TMPTE	29	1.2
TETA/TMPTE	41	3.0

Table 4: Results of interdiffusion experiments in microcalorimetry: ratio of the heat of reaction for layered healing agents versus the heat of reaction for mixed healing agents, and thickness of the solid layer formed after interdiffusion and reaction.

As the ratio of the heat of reaction for unmixed and mixed systems is similar for JEFF D230/PPGDE and TETA/TMPTE, a similar thickness of the solid layer might be expected. However, this is not the case due to the difference in functionality of the amines and epoxies, 6 for TETA, 4 for JEFF D230, 3 for TMPTE and 2 for PPGDE, which leads to a difference in gel conversion. According to the Flory-Stockmayer equation [41,42], for JEFF D230/PPGDE, a 4+2 system, the gel conversion is estimated to be 0.58, while for TETA/TMPTE, a 6+3 system, the gel conversion is 0.32. This means that, for TETA/TMPTE, gelation will take place at a much lower conversion forming a thicker layer. These experiments show that the studied systems were sufficiently slow at 25 °C to allow for interdiffusion of amine and epoxy over 1 mm and more before the diffusion was blocked by the network formed. Although the vascular systems developed in this work are mainly oriented towards the healing of microcracks at an early stage of failure, these amine/epoxy systems have the capability of healing even mm-wide cracks in damaged composite matrices, in the absence of active mixing, if enough healing agent can be transported to the crack.

4.4 Infusion

The uptake of the epoxies and amines in, and their transport through, the vascular network through capillary forces was monitored for seven days by gravimetry. An overlay of the mass uptake curves for samples infused with TMPTE and JEFF D400, respectively, is shown in Figure 5. It can be seen that the final mass uptake is similar for the two components. Three distinct regimes can be noticed for both healing agents. A first regime showing a rapid uptake of about 20 mg (Figure 5a), a second regime showing a more gradual uptake up to about 75 mg (linear on the $t^{1/2}$ scale in Figure 5b), and a further slow increase to a plateau value at about 90 mg. With FTIR, it was proven that there is wicking at the outside of the sample (Figure 6). The FTIR spectrum of the infused sample was taken at a position that was not immersed in the healing agent during the wicking of the sample. To check the rate of uptake at the outside and the absorption through the surfaces in direct contact with the liquid, the wicking experiment was also performed on a virgin epoxy sample (without vascular network) using TMPTE (Figure 5). In this case, the uptake of mass is limited and does not correspond to the rapid initial increase seen for the samples with channels. It is thus probable that the first rapid increase corresponds to the uptake in larger channels, the second fast increase to the uptake of healing agent in channels with a smaller diameter, and the third slow increase to the wicking at the outside of the sample and/or the absorption into the matrix, which occurs at a much lower rate, and will thus take much more time. Of course, the absorption into the matrix is expected to be faster in case of the samples with channels, because the specific contact area is much larger and even increases once the channels get filled. Based on this, it can be assumed that the samples are completely infused after less than two days for a sample height of 4 cm.

FIGURE 5 (double column)

FIGURE 6 (single column)

During the infusion experiments with JEFF D230 and TETA, the samples were damaged: the sample infused with JEFF D230 was cracked and visibly swollen, while the sample infused with TETA was shattered into multiple pieces. This is attributed to the absorption of TETA and JEFF D230 into the thermoset matrix, the (local) swelling of the network causing internal stresses, in combination with the capillary pressure exerted by the healing agent in the channels. In addition, it was noticed that the samples infused with TETA, JEFF D230 and JEFF D400 became rubbery. The healing agents clearly act as plasticizers, decreasing T_g. Swelling tests on samples of 23 mm by 3.1 mm by 0.6 mm confirmed that most of the selected healing agents diffuse into the polymer matrix and swell it significantly leading to vulome changes of 1.1 vol% to 4.3 vol%. A limited swelling might be beneficial for crack closure and improved adhesion between the healing system and the epoxy matrix, however, too extensive swelling (>1%) clearly jeopardizes the integrity of the matrix.

These results show that TETA and JEFF D230 are not suitable as healing agents in a vascular self-healing application where the healing agents are in contact with the matrix. If the healing agents were separated from the matrix by an impervious layer, those amines could still be used. Such a structure could be achieved by co-axial electrospinning, which allows making fibrous tubes filled with liquid healing agents (a core-shell system). Coaxial electrospinning has already been successfully used to make a vascular network for use in a self-healing

application by Lee et al. [43,44], using a healing chemistry based on siloxanes. Aside from separating healing agent and matrix prior to damage, a major benefit of coaxial electrospinning is that the dissolution of the sacrificial fibres and the infusion of the healing agents into the channels are no longer needed, which makes it more easily up-scalable to larger composites parts. Hence, despite the fact that TETA and JEFF D230 are not suitable for the vascular self-healing application based on sacrificial fibres, the four studied healing systems were still used to determine the influence of $T_{g\ x=1}$ on the healing capability, as they could be used in other self-healing strategies.

4.5 Healing capability

To test the healing capability of the different healing systems, samples of the original epoxy thermoset without vascular network were broken and glued back together with the selected healing systems. The samples were cured at RT for 7 days and were then tested using three-point-bending. The healing capability is calculated by taking the ratio of the peak load for the samples healed with the amine/epoxy system over the peak load of samples healed with the original matrix mixture (reference) and fully cured. Figure 7 shows that the higher the $T_{g\ x=1}$ of the amine/epoxy system, the higher the healing capability. Note that using the original matrix resin results in the highest strength of the repaired sample (the efficiencies of all other systems are lower), however, the much higher viscosity of its components makes them unsuitable as healing agents in a vascular approach.

FIGURE 7 (single column)

After the three-point-bending tests, the surfaces of the broken samples were analysed under an optical microscope (Figure 8). For all systems it could be seen that the facture was within the layer of healing agents, and thus that for all systems cohesive fracture led to the failure of the samples. The difference in texture of the healing agent layer is linked to the difference in glass transition temperature. TETA/TMPTE has a T_g above ambient temperature, so is in the glassy state and thus shows a more brittle fracture. Thus, the increase in healing capability with $T_{g\ x=1}$ can be attributed to a higher crosslink density resulting in an increased mechanical strength of the cured healing system. The good adhesion of all healing systems to the original matrix is probably due to the partial absorption of the healing agents by the matrix and the formation of interpenetrating and covalently linked structures.

FIGURE 8 (double column)

5. CONCLUSIONS

The suitability of several two-component healing systems for the self-healing of a vascularized epoxy thermoset prepared using sacrificial electrospun fibres was investigated by evaluating their infusion in the channels, the degree to which they swell the matrix, their

interdiffusion and reaction kinetics, and their repair quality. Upon selecting and evaluating such healing systems, the interactions between the healing agents and the matrix clearly needs to be considered at a very early stage. On the one hand, if the two are too compatible, too extensive swelling may cause complete failure of the original thermoset. On the other hand, limited diffusion of the healing agents into the matrix, and the swelling inherently connected to it, might be beneficial for crack closure and for an improved adhesion between the healing system and the epoxy matrix. For all healing systems studied, interdiffusion and reaction occurred over distances larger than 1 mm, indicating that the presented healing systems are suitable for healing microcracks and even mm-scale damage.

For the systems tested, the best healing performance is observed for TETA/TMPTE, the system having the highest $T_{g\ x=1}$ at full cure, but a too extensive swelling of the matrix prevents its application in vascularized epoxy thermosets prepared using sacrificial electrospun fibres. The contradictory requirements of (1) no or limited swelling for preserving the integrity of the matrix and (2) good compatibility to ensure adhesion, combined with the time-consuming steps of fibre dissolution and infusion of the healing agents, make the vascular self-healing systems based on sacrificial electrospun fibres less suitable for upscaling to an industrial level. However, the development of vascular self-healing thermosets using coaxial electrospun fibres that contain the healing agents in the core of separately spun fibres, would address these issues.

6. ACKNOWLEDGEMENTS

The authors would like to acknowledge the VUB for a grant for Audrey Cuvellier and Frans Boulpaep of the department Mechanics of Materials and Constructions (VUB) for his help with the three point bending tests.

REFERENCES

[1] S.R. White, B.J. Blaiszik, S.L.B. Kramer, S.C. Olugebefola, J.S. Moore, N.R. Sottos, Self-healing Polymers and Composites Capsules , circulatory systems and chemistry allow materials to fix themselves, Am. Sci. 99 (2011) 392–399. doi:10.1511/2011.92.392.

[2] E.B. Murphy, F. Wudl, The world of smart healable materials, Prog. Polym. Sci. 35 (2010) 223–251. doi:10.1016/j.progpolymsci.2009.10.006.

[3] S.R. White, N.R. Sottos, P.H. Geubelle, M.R. Kessler, S.R. Sriram, E.N. Brown, S. Viswanathan, Autonomic healing of polymer composites, Nature. 409 (2001) 794–797. doi:10.1038/415817a.

[4] S.H. Cho, H.M. Andersson, S.R. White, N.R. Sottos, P. V. Braun, Polydiniethylsiloxane-based self-healing materials, Adv. Mater. 18 (2006) 997–1000. doi:10.1002/adma.200501814.

[5] B.J. Blaiszik, N.R. Sottos, S.R. White, Nanocapsules for self-healing materials, Compos. Sci. Technol. 68 (2008) 978–986. doi:10.1016/j.compscitech.2007.07.021.

[6] Y. Jinglei, M.W. Keller, J.S. Moore, S.R. White, N.R. Sottos, Microencapsulation of isocyanates for self-healing polymers, Macromolecules. 41 (2008) 9650–9655. doi:10.1021/ma801718v.

[7] H. Jin, C.L. Mangun, D.S. Stradley, J.S. Moore, N.R. Sottos, S.R. White, Self-healing thermoset using encapsulated epoxy-amine healing chemistry, Polymer (Guildf). 53 (2012) 581–587. doi:10.1016/j.polymer.2011.12.005.
[8] H. Zhang, J. Yang, Development of self-healing polymers via amine–epoxy chemistry: II. Systematic evaluation of self-healing performance, Smart Mater. Struct. 23 (2014) 065004. doi:10.1088/0964-1726/23/6/065004.
[9] M. Motuku, U.K. Vaidya, G.M. Janowski, Parametric studies on self-repairing approaches for resin infused composites subjected to low velocity impact, Smart Mater. Struct. 8 (1999) 623–638. doi:10.1088/0964-1726/8/5/313.
[10] R.S. Trask, I.P. Bond, Biomimetic self-healing of advanced composite structures using hollow glass fibres, Smart Mater. Struct. 15 (2006) 704–710. doi:10.1098/rsif.2006.0194.
[11] R.. Trask, G.. Williams, I.. Bond, Bioinspired self-healing of advanced composite structures using hollow glass fibres, J. R. Soc. Interface. 4 (2007) 363 –371. doi:10.1098/rsif.2006.0194.
[12] K.S. Toohey, N.R. Sottos, J. a. Lewis, J.S. Moore, S.R. White, Self-healing materials with microvascular networks, Nat. Mater. 6 (2007) 581–585. doi:10.1038/nmat1934.
[13] A.R. Hamilton, N.R. Sottos, S.R. White, Mitigation of fatigue damage in self-healing vascular materials, Polymer (Guildf). 53 (2012) 5575–5581. doi:10.1016/j.polymer.2012.09.050.
[14] C. Chen, K. Peters, Y. Li, Self-healing sandwich structures incorporating an interfacial layer with vascular network, Smart Mater. Struct. 22 (2013) 025031. doi:10.1088/0964-1726/22/2/025031.
[15] J.F. Patrick, K.R. Hart, B.P. Krull, C.E. Diesendruck, J.S. Moore, S.R. White, N.R. Sottos, Continuous self-healing life cycle in vascularized structural composites, Adv. Mater. 26 (2014) 4302–4308. doi:10.1002/adma.201400248.
[16] M. Zhang, M. Rong, Design and synthesis of self-healing polymers, Sci. China Chem. 55 (2012) 648–676. doi:10.1007/s11426-012-4511-3.
[17] X. Chen, F. Wudl, A.K. Mal, H. Shen, S.R. Nutt, New Thermally Remendable Highly Cross-Linked Polymeric Materials New, Macromolecules. 36 (2003) 1802–1807. doi:10.1021/ma0210675.
[18] D.H. Turkenburg, H.R. Fischer, Diels-Alder based, thermo-reversible cross-linked epoxies for use in self-healing composites, Polymer (Guildf). 79 (2015) 187–194. doi:10.1016/j.polymer.2015.10.031.
[19] C.M. Chung, Y.S. Roh, S.Y. Cho, J.G. Kim, Crack healing in polymeric materials via photochemical [2+2] cycloaddition, Chem. Mater. 16 (2004) 3982–3984. doi:10.1021/cm049394+.
[20] L. Hu, X. Cheng, A. Zhang, A facile method to prepare UV light-triggered self-healing polyphosphazenes, J. Mater. Sci. 50 (2015) 2239–2246. doi:10.1007/s10853-014-8786-y.
[21] B. Aïssa, D. Therriault, E. Haddad, W. Jamroz, Self-Healing Materials Systems : Overview of Major, Adv. Mater. Sci. Eng. 2012 (2012) 1–17. doi:10.1155/2012/854203.
[22] K.S. Toohey, N.R. Sottos, S.R. White, Characterization of Microvascular-Based Self-healing Coatings, Exp. Mech. 49 (2008) 707–717. doi:10.1007/s11340-008-9176-7.
[23] E.N. Brown, M.R. Kessler, N.R. Sottos, S.R. White, In situ poly (urea-formaldehyde) microencapsulation of dicyclopentadiene, J. Microencapsul. 20 (2003) 719–730. doi:10.1080/0265204031000154160.
[24] X.F. Wu, A.L. Yarin, Recent progress in interfacial toughening and damage self-healing of polymer composites based on electrospun and solution-blown nanofibers:

An overview, J. Appl. Polym. Sci. 130 (2013) 2225–2237. doi:10.1002/app.39282.
[25] R.S. Trask, H.R. Williams, I.P. Bond, Self-healing polymer composites: mimicking nature to enhance performance., Bioinspir. Biomim. 2 (2007) 1–9. doi:10.1088/1748-3182/2/1/P01.
[26] A.P. Esser-Kahn, P.R. Thakre, H. Dong, J.F. Patrick, V.K. Vlasko-Vlasov, N.R. Sottos, J.S. Moore, S.R. White, Three-Dimensional Microvascular Fiber-Reinforced Composites, Adv. Mater. 23 (2011) 3654–3658. doi:10.1002/adma.201100933.
[27] H.R. Williams, R.S. Trask, I.P. Bond, Self-healing composite sandwich structures, Vascular. 16 (2007) 1198–1207. doi:10.1088/0964-1726/16/4/031.
[28] H. Zhang, J. Yang, Development of self-healing polymers via amine–epoxy chemistry: II. Systematic evaluation of self-healing performance, Smart Mater. Struct. 23 (2014) 065004. doi:10.1088/0964-1726/23/6/065004.
[29] K.S. Toohey, C.J. Hansen, J.A. Lewis, S.R. White, N.R. Sottos, Delivery of two-part self-healing chemistry via microvascular networks, Adv. Funct. Mater. 19 (2009) 1399–1405. doi:10.1002/adfm.200801824.
[30] A. Torre-Muruzabal, L. Daelemans, G. Van Assche, K. De Clerck, H. Rahier, Creation of a nanovascular network by electrospun sacrificial nanofibers for self-healing applications and its effect on the flexural properties of the bulk material, Polym. Test. 54 (2016) 78–83. doi:10.1016/j.polymertesting.2016.06.026.
[31] ISO, Plastics. Determination of flexural properties, 5 (2010). doi:10.3403/30188331.
[32] G. Van Assche, A. Van Hemelrijck, H. Rahier, B. Van Mele, Modulated differential scanning calorimetry: isothermal cure and vitrification of thermosetting systems, Thermochim. Acta. 268 (1995) 121–142. doi:10.1016/0040-6031(95)02693-2.
[33] F. Meyer, G. Sanz, A. Eceiza, I. Mondragon, J. Mijovic, The effect of stoichiometry and thermal history during cure on structure and properties of epoxy networks, Polymer (Guildf). 36 (1995) 1407–1414. doi:10.1016/0032-3861(95)95918-Q.
[34] Y.-H. Lin, Polymer Viscoelasticity, 2nd ed., 2010. doi:10.1142/9789814313049.
[35] W. Callister, D. Rethwisch, Materials science and engineering: an introduction, 2007. doi:10.1016/0025-5416(87)90343-0.
[36] J.T. Seitz, The estimation of mechanical properties of polymers from molecular structure, J. Appl. Polym. Sci. 49 (1993) 1331–1351. doi:10.1002/app.1993.070490802.
[37] D.J. O'Brien, N.R. Sottos, S.R. White, Cure-dependent viscoelastic poisson's ratio of epoxy, Exp. Mech. 47 (2007) 237–249. doi:10.1007/s11340-006-9013-9.
[38] H.J. Flammersheim, Typical sources of error in the kinetic analysis of models with pre-equilibria: DSC investigations of epoxide-amine curing reactions, Thermochim. Acta. 296 (1997) 155–159. doi:10.1016/S0040-6031(97)00113-5.
[39] J. Lee, M. Shim, S. Kim, Effect of modified rubber compound on the cure kinetics of DGEBA / MDA system by Kissinger and isoconversional methods, Thermochim. Acta. 371 (2001) 6–12. doi:10.1016/S0040-6031(00)00771-1.
[40] S. Swier, B. Van Mele, Reaction thermodynamics of amine-cured epoxy systems: Validation of the enthalpy and heat capacity of reaction as determined by modulated temperature differential scanning calorimetry, J. Polym. Sci. Part B Polym. Phys. 41 (2003) 594–608. doi:10.1002/polb.10413.
[41] J. Flory, Molecular distribution in three dimensional polymers, J. Am. Chem. Soc. 63 (1941) 3083–3090. doi:10.1021/ja01856a061.
[42] W.H. Stockmayer, Theory of molecular size distribution and gel formation in branched-chain polymers, J. Chem. Phys. 11 (1943) 45. doi:10.1063/1.1723803.
[43] M.W. Lee, S. An, C. Lee, M. Liou, A.L. Yarin, S.S. Yoon, Self-healing transparent core–shell nanofiber coatings for anti-corrosive protection, J. Mater. Chem. A. 2 (2014)

7045–7053. doi:10.1039/c4ta00623b.
[44] M.W. Lee, S. An, H.S. Jo, S.S. Yoon, A.L. Yarin, Self-Healing Nanofiber-Reinforced Polymer Composites. 1. Tensile Testing and Recovery of Mechanical Properties, ACS Appl. Mater. Interfaces. 7 (2015) 19546−19554. doi:10.1021/acsami.5b05998.

Figure 1: SEM images of the cross sections of the submicron channels in the vascularised epoxy samples at different magnifications. The interconnections between parallel and perpendicular submicron channels can be seen in squares and circles, respectively.

Figure 2: Schematic representation of the interdiffusion experiment with the amine (light gray) gently deposited on top of the epoxy (black). Due to diffusion and reaction a solid layer is formed (dark gray).

Figure 3: T_g at full cure for different amine/epoxy ratios measured with DMA based on the maximum in tan delta for a) JEFF D230/PPGDE, b) JEFF D400/TMPTE, c) JEFF D230/TMPTE and d) TETA/TMPTE. The width of T_g is determined based on onset and offset temperatures of tan delta.

Figure 4: Heat flow curves for the different healing systems at 25 °C for a stoichiometric amine/epoxy ratio.

Figure 5: Mass uptake of epoxy samples of which the bottom is immersed into the healing agents: uptake for samples with a vascular network in JEFF D400 (black) and TMPTE (light grey) and for a virgin epoxy sample in TMTPE dark grey. a) Zoom on the first hour, b) Experiment over 7 days plotted on a $t^{1/2}$ scale.

Figure 6: FTIR measurements of the healing agent (black), of the infused sample at a position that was not immersed in the healing agent during the wicking experiment (dark grey) and of what was left on the FTIR sensor after removal of the infused sample (light grey)

Figure 7: The healing capability as a function of the $T_{g\,x=1}$ of the healing systems and reference (η=100%).

Figure 8: Optical microscope images of the fracture planes of the glued samples after three point bending tests. From left to right: JEFF D230/PPGDE, JEFF D400/TMPTE, JEFF D230/TMPTE and TETA/TMPTE.